Natural DIAMOND Mistaken as HPHT Synthetic

When a declared synthetic diamond is submitted to a GIA laboratory, it is not often that the diamond turns out to be natural. But this was the case recently when a D-color 2.23 ct round brilliant was submitted to the Carlsbad laboratory for a synthetic diamond grading report (figure 1). Its infrared absorption spectrum established it as type IaA>B, with nitrogen aggregates around 80 ppm, confirming a natural color origin. Since it was stated as synthetic, further analysis was performed.

There are very few gemological indicators of lab-grown diamonds (S. Eaton-Magaña and C.M. Breeding, "Features of synthetic diamonds," Summer 2018 *G&G*, pp. 202–204). Yet one of the most reliable and easily seen observations is the lack of birefringence (or strain) patterns in HPHT synthetics when viewed between crossed polarizers. To our knowledge, visible strain in HPHT-grown synthetic diamonds has only been documented in one rare case (Winter 2016 Lab Notes, pp. 417–418).

Although strain observations are rarely used by many in the trade, this natural diamond was perhaps presumed to be synthetic due to its apparent lack of observable strain. When viewed under crossed polarizers, the strain was very difficult to discern (figure 2, left), and this apparent absence was consistent with our observations of HPHT synthetics. With extensive searching and careful positioning, the strain was visible in a few scattered areas of the diamond. The observed strain was linear in appearance, consistent with type Ia natural diamonds (figure 2, right).

Figure 1. This D-color 2.23 ct natural diamond was originally submitted as a synthetic.

With further investigation using a variety of techniques such as photoluminescence spectroscopy and DiamondView imaging, all tests confirmed a natural origin. Additionally, microscopic observation revealed unidentified dark natural crystal inclusions (figure 3), which might have been mistaken for metallic flux.

Subsequently the client indicated that this stone was believed to be synthetic after examination by another party in the trade. However, several gemological and spectroscopic tests confirmed its natural origin.

This diamond demonstrates why stones of uncertain origin should be submitted to a gemological laboratory for further testing. It also provides confirmation that occasional exce-

Figure 2. An apparent lack of strain was observed throughout most of the stone, with strain visible only around inclusions (left). Such observations are common in HPHT synthetics and not generally seen in natural or CVD synthetic diamonds. With extensive searching and careful positioning, linear strain was visible within small areas of the stone (right). Field of view 7.19 mm.

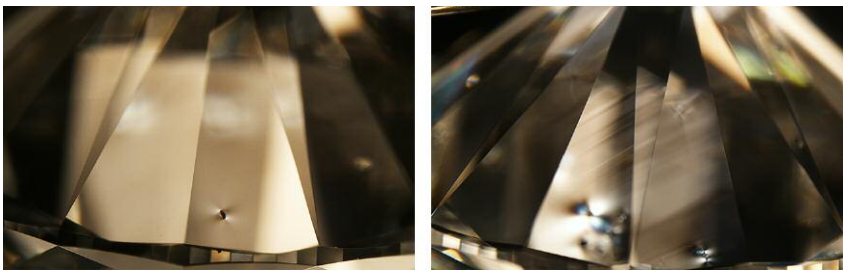

Editors' note: All items were written by staff members of GIA laboratories.

GEMS & GEMOLOGY, Vol. 54, No. 4, pp. 430–439.

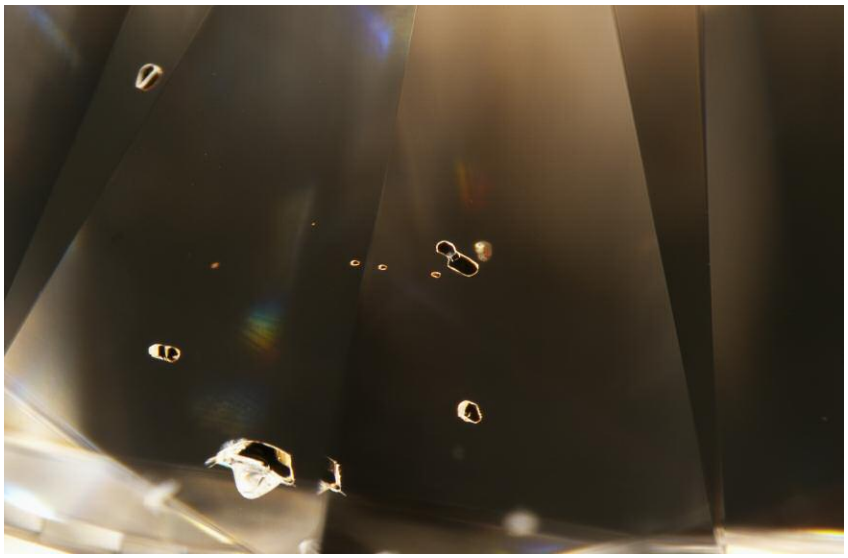

Figure 3. Microscopic examination shows discernible dark mineral inclusions that occur naturally in diamonds and could have been mistaken for metallic flux inclusions. Field of view 3.57 mm.

tions exist for the general guidelines that help distinguish natural from lab-grown diamonds. In this case, the correction worked to the client's advantage.

Garrett McElhenny and Sally Eaton-Magaña

Manufactured GOLD-IN-QUARTZ Jewelry

Due to its desirability, gold is often imitated with minerals such as pyrite or with gold plating. Gold occurs in small quantities in many kinds of rocks throughout the world. It is typically found in epithermal deposits where hydrothermal fluids deposit gold, along with pyrite and other sulfides, into cracks and faults of rocks—commonly quartz-bearing rocks (J.W. Anthony et al., *Handbook of Mineralogy, Vol. 1: Elements, Sulfides, Sulfosalts*, Mineral Data Publishing, Tucson, Arizona, 1990). Due to the aggregate structure of this material, the gold contained in natural gold-in-quartz is deposited irregularly, showing a more natural-looking sporadic veining system in the host quartz (figure 4).

The Carlsbad lab was recently sent three jewelry pieces—two bracelets and a ring—for identification reports (figure 5). The ring and one of the bracelets were set with numerous white stones cross-cut with yellow metallic veins. One bracelet had black stones cross-cut with similar yellow metallic veining. Standard gemological testing of both the white and black stones revealed properties consistent with quartz; these results were confirmed with Raman spectroscopy. The Raman analysis of the black stones indicated the presence of amorphous carbon, which drew some suspicion.

These jewelry pieces initially seemed to contain natural gold-in-quartz. Upon further inspection, the yellow metallic veining system appeared inorganic in the host quartz due to its very consistent appearance in all the stones. In the three pieces, the metallic veins had a spiderweb-like structure, and a colorless polymer was also present alongside the metallic veins (figure 6, left). The colorless polymer areas also showed undercutting, and the metallic veining had areas of incomplete filling (figure 6, center and right). These features were consistent with the manufactured gold-in-quartz products that were first introduced to the market at the 2005 Tucson shows (B. Laurs, "Manufactured gold/silver-in-quartz," Spring 2005 *G&G*, pp. 63–64). This material was composed of polymer, quartz, and metallic veining similar to what was observed in the stones we examined. Even with the slight difference in the face-up appearance of the natural and manufactured gold-in-quartz, the manufacturer claims that the only way to clearly distinguish this imitation material is with chemical analysis of the metal alloy.

Figure 4. The gold veins in natural gold-in-quartz are irregular and show a natural nugget structure below the surface. Field of view 4.79 mm.

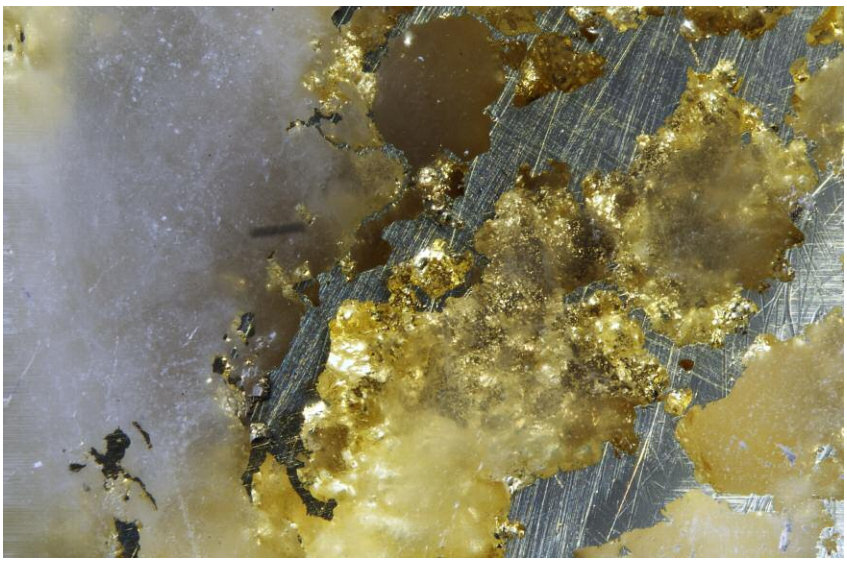

Figure 5. Manufactured gold-in-quartz, set in two bracelets and a ring that were submitted for identification reports.

Laser ablation–inductively coupled plasma–mass spectrometry (LA-ICP-MS) analyses were performed on the yellow metallic veins in the white and black stones of each bracelet to further separate them from natural gold-in-quartz. Each ablation spot was drilled twice into the veins. The chemistry of the first spot was very similar for the stones in both bracelets. The vein was mainly composed of gold (Au) and silver (Ag) with traces of nickel (0.90–2.67 parts per million weight, ppmw) and copper (23.58–30.02 ppmw). The gold to silver weight ratio (Au_{ppmw}/Ag_{ppmw}) was between 2.71 and 3.33. The chemistry of the second spot on the same position showed little gold or silver and a significant amount of silica, which indicated that the laser had passed through the yellow metallic layer and into the host quartz below.

One natural gold-in-quartz cabochon obtained from the GIA Museum was analyzed for comparison. The veins found in the natural sample (again, see figure 4) were composed mainly of yellow metallic materials, with additional gray metallic minerals. The same experimental procedures were applied to both the yellow and gray areas. The chemistry of the gray metallic areas identified them as an iron sulfide mineral. The chemistry of the first spot on a yellow metallic area showed a large amount of gold and silver with traces of copper (215–257 ppmw). The gold and silver weight ratio (Au_{ppmw}/Ag_{ppmw}) was between 7.84 and 8.04. It was evident that the concentration of gold in the yellow metallic veins in the natural gold-in-quartz was much higher than that of the yellow metallic veins in the white and black panels of the two bracelets. In addition, the natural veins had a higher copper concentration than the two bracelets.

The manufactured gold-in-quartz materials first reported in 2005 are still circulating in the market today. Consumers should be aware of this when purchasing pieces reported to contain gold-in-quartz. The telling indicator of manufactured gold-in-quartz is the consistent texture of its yellow metallic veins. The gold in the natural version is much more sporadic and appears as chunky conglomerated nuggets.

Nicole Ahline and Ziyin Sun

Freshwater PEARLS, Blister and Loose, with Their Host Shells

GIA occasionally receives blister pearls attached to their host shells for identification (Winter 2015 Lab Notes, pp. 432–434; Summer 2017 Lab Notes, pp. 231–232), which can provide helpful information on the overall growth conditions and the mollusk species. Recently the New York laboratory had an opportunity to study three freshwater specimens: two blister pearls still attached to their shells, and one loose "wing" pearl that was reportedly

Figure 6. Unnatural veins in manufactured gold-in-quartz. Left: This vein is filled with both polymer, which is not flush with the host quartz, and gold (field of view 4.79 mm). Center: A vein of polymer running alongside a vein of gold with undercutting visible at the boundary of the polymer vein and the host quartz (field of view 3.57 mm). Right: Polymer fills an incomplete gold vein; the rest of the vein is recessed below the host quartz (field of view 7.19 mm).

Figure 7. Three freshwater pearls attached to their host shells. Left to right: A blister pearl measuring approximately 37.45 × 27.48 mm, a loose wing pearl measuring 35.82 × 9.37 × 5.94 mm and weighing 10.60 ct, and a blister pearl measuring approximately 23.60 × 19.49 mm. Specimens courtesy of Mississippi River Pearl Jewelry Co. LLC.

found in the shell with which it was submitted (figure 7).

While approximately 1,000 species of freshwater mussels have been identified worldwide, the United States alone is said to host about 300 species, compared to 96 species in Africa, 60 in China, and 12 in Europe (Virginia Department of Game and Inland Fisheries, 2018, https://www.dgif.virginia.gov/wildlife/freshwater-mussels/). The number of U.S. species shows the spectacular diversity of its freshwater resources. Hence, it proves how difficult it can be to apply correct zoological names to specific shells. However, experienced local fishermen who harvest the mussels are often the source of helpful information (T. Hsu et al., "Freshwater pearling in Tennessee," 2016, https://www.gia.edu/gia-news-research/freshwater-pearling-tennessee). The owner claimed that the loose wing-shaped pearl (figure 7, center) was found in a *Potamilus purpuratus* "Bluefer" mussel in a U.S. river. Bluefer mussels exhibit a pinkish purple to deep purple nacre lining and can produce pearls of a similar color range. Energy-dispersive X-ray fluorescence (EDXRF) spectrometry confirmed that it originated from a freshwater environment, based on its chemistry result of more than 1000 ppmw manganese. Freshwater pearls usually show higher than 100 ppmw manganese content. Real-time X-ray microradiography (RTX) revealed a natural growth structure, while Raman spectroscopy detected aragonite and polyenic peaks, the latter indicating the presence of natural coloring pigments (S. Karampelas et al., "Role of polyenes in the coloration of cultured freshwater pearls," *European Journal of Mineralogy*, Vol. 21, 2009, pp. 85–97). This specimen also displayed the characteristic elongated, flat, and slightly curved shape characteristic of wing pearls that, as the name implies, resembles the shape of a bird's wing. Wing pearls commonly form in the hinge area within shells, and it was interesting to see a similar-sized cavity in the shell submitted with this pearl.

The other two blister pearls were also claimed to have originated from a freshwater environment, and this was confirmed by their optical X-ray fluorescence reactions. Both specimens showed a strong yellowish green luminescence under X-ray excitation, a result that agrees with pearls from a freshwater environment due to their higher manganese content (H.A. Hänni et al., "X-ray luminescence, a valuable test in pearl identification," *The Journal of Gemmology*, Vol 29, No. 5/6, 2005, pp. 325–329). According to the owner, the smaller shell (figure 7, right), possibly a washboard mussel (*Megalonaias nervosa*), was found in a U.S. river, while the larger shell (figure 7, left) is likely a hybrid *Hyriopsis* mussel commonly used by cultured pearl farmers in China. Blister pearls form when a whole pearl within the connective tissue breaks through the mantle due to its size and/or weight, or for some other reason, and presses against the nacreous inner surface of the shell, where subsequent nacre deposition fuses the pearl to the shell (E. Strack, *Pearls*, Ruhle-Diebener-Verlag, Stuttgart, Germany, 2006, p. 124).

The size of these two blister pearls is impressive, and both protrude conspicuously from the shell while still attached to their hosts (figure 8). The RTX results of the smaller blister

Figure 8. Close-up images of the freshwater blister pearls from China (left) and the United States (right) attached to their hosts.

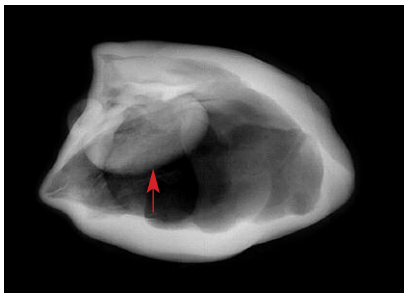

Figure 9. The RTX structure of the large blister pearl (shown on the left in figures 7 and 8) revealed a void-like structure in which a near-oval feature is visible (indicated by the arrow).

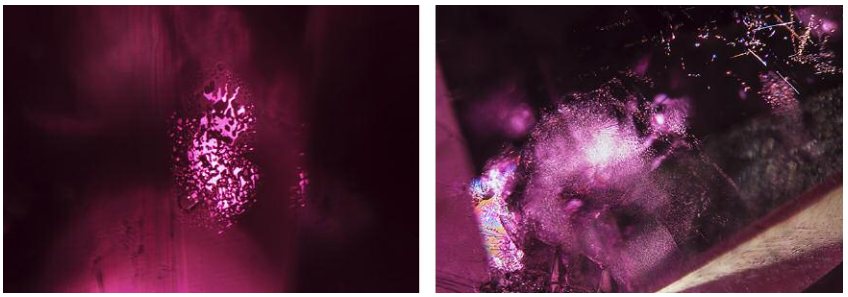

Figure 10. Inclusions in the 1.70 ct ruby from Montana. Left: Close-up of a glassy melt inclusion with an associated thin film showing geometric patterns; field of view 1.76 mm. Right: A melt inclusion with an iridescent thin film, partial hexagonal zone of particles, and short needles; field of view 3.81 mm.

pearl revealed concentric growth arcs proving its natural origin. However, the RTX results of the larger blister pearl revealed a void-like structure that may be found within natural and non-bead-cultured pearls, but a near-oval feature inside the void is uncommon in natural pearls (figure 9). GIA gemologists believe this oval feature was the triggering mechanism that likely resulted in the formation of the blister pearl. Whether this oval feature is a by-product of pearl culturing or a natural formation is hard to prove without examining the blister pearl thoroughly in other orientations, which was precluded by its size and position. While the identification of some freshwater pearls remains challenging, these known freshwater samples together with their host shells serve as useful references for laboratory gemologists.

Joyce Wing Yan Ho

A Rare RUBY from Montana

The Carlsbad laboratory recently received a 1.70 ct purplish red octagonal modified brilliant-cut ruby measuring 6.28 × 6.25 × 4.56 mm for an identification and origin report. Standard gemological testing gave a chromium spectrum indicating ruby and a hydrostatic SG of 4.00. The stone displayed a weak red fluorescence in long-wave UV and no fluorescence under short-wave UV.

Microscopic examination showed an interesting combination of inclusions (figure 10). There were several glassy melt inclusions and small crystals with associated reflective thin films. The thin films often displayed hexagonal geometric patterns conforming to the crystallographic orientation of the host ruby. These resembled the patterns commonly seen in rubies from Thailand and Cambodia and have also been documented in Montana corundum (Fall 2015 *G&G* Micro-World, pp. 329–330). A partial hexagonal zone of particles and more loosely spaced unaltered exsolved rutile needles was also present, a feature that would be very unusual in Thai/Cambodian rubies. A large intact colorless crystal as well as smaller white crystals were located deep within the stone, so we were unable to conclusively identify them with Raman spectroscopy. This inclusion scene is consistent with unheated corundum from Montana.

LA-ICP-MS was used to determine the stone's trace-element chemistry,

Figure 11. The 1.70 ct Montana ruby alongside rough pink to purple corundum samples from the GIA reference collection. These reference samples, collected from Montana's Eldorado Bar along the Missouri River and Wildcat Gulch, part of the Rock Creek deposit, were used to help determine the country of origin.

and the results were compared to corundum samples from GIA's colored stone reference collection. Trace element measurements indicated ranges of 15.1–17.2 ppma Mg, 14.7–16.9 ppma Ti, 3.67–3.87 ppma V, 359–406 ppma Cr, 1500–1580 ppma Fe, and 14.6–14.7 ppma Ga. The chemistry matched well with reference stones GIA has collected from Montana's secondary deposits (figure 11) but not our Thai/Cambodian ruby reference samples. In particular, Thai/Cambodian rubies tend to have higher Mg (often above 100 ppma), while this stone had much lower Mg levels.

Montana's secondary deposits produce sapphires in a wide range of mostly pastel colors. Pink corundum tends to be rarer than blue or green, and those that possess the depth of color to be called ruby are quite rare, particularly without any treatments. The color, combined with the large size, makes the 1.70 ct ruby from Montana an exceptional specimen—this is only the second such report issued by the lab to date. With a combination of microscopic observation, advanced testing methods, and GIA's reference collection, we were able to confirm the country of origin.

Claire Malaquias

Large Pargasite Inclusion in Kashmir SAPPHIRE

Kashmir sapphires are known to have occurred in kaolinized plagioclase feldspar pegmatites, found as pockets between metamorphic stratified beds/cliffs of the Himalayan Zanskar Range. These sapphires captured many cognate mineral inclusions—such as pargasite, plagioclase feldspar, tourmaline, and zircon—which demarcate the pockets against the country rock (E.J. Gübelin and J.I. Koivula, *Photoatlas of Inclusions in Gemstones*, Vol. 3, Opinio Publishers, Basel, Switzerland, 2008, p. 194).

Pargasite mineral inclusions (prismatic or as long, fine needles) in blue sapphire are regarded as a strong indicator of Kashmir origin. (R. Schwieger, "Diagnostic features and heat treatment of Kashmir sapphires," Winter 1990 *G&G*, pp. 267–280).

Recently, a 14.06 ct octagonal-cut blue sapphire (figure 12) submitted to GIA's Carlsbad laboratory for origin determination was of particular interest for its several unusually large, eye-visible pargasite crystal inclusions. Standard gemological properties confirmed the host sapphire's identity, and advanced analytical testing specified its metamorphic geological origin.

Microscopic examination revealed an inclusion scene reminiscent of "new Kashmir," a term referring to Kashmir sapphires that have come into the market since the 2000s. The blue sapphire featured several negative crystals, black graphite inclusions, unidentified rounded and needle-shaped colorless crystal inclusions (probably slender zircon rods or pargasite), reflective thin films, and fluid fingerprints.

Classic Kashmir sapphire features were also observed, such as "milky" turbid whitish broad bands, clouds, a parallel chromium-enriched zone (which glows red under long-wave UV illumination), ladder-like/antenna-like stringers, and snowflake-like inclusions.

Figure 12. This 14.06 ct octagonal blue Kashmir sapphire exhibits large, eye-visible inclusions of prismatic pargasite.

The main inclusion features, the pargasite crystals (figure 13), were transparent with a brownish green bodycolor. Many of them were doubly terminated with a flat, columnar prismatic morphology with striations along their length, surrounded by halo- or rosette-like thin reflective

Figure 13. A large prismatic pargasite mineral inclusion. Field of view 7.19 mm.

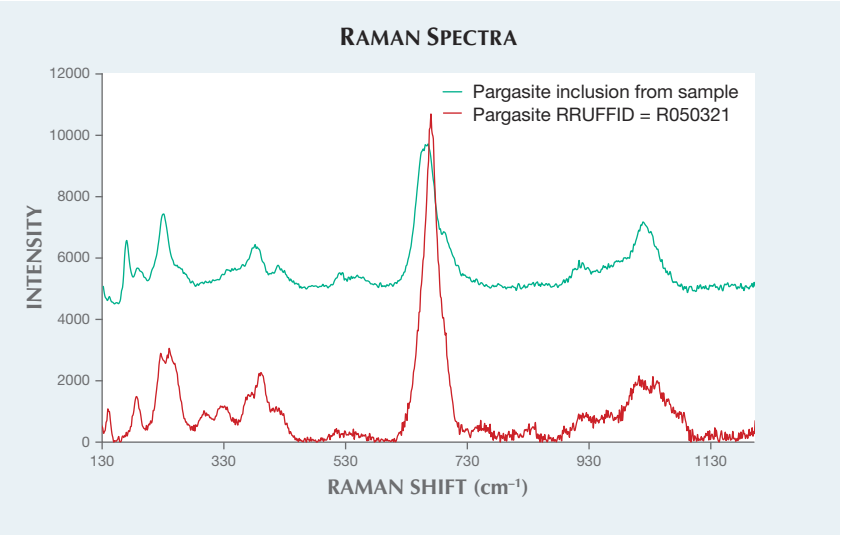

Figure 14. Unoriented Raman spectra with 514 nm excitation confirmed the pargasite mineral inclusion identity (blue spectrum), using the RRUFF database as a reference (red spectrum).

films. The pargasite crystal's surface pits and altered appearance suggested that these pargasite crystals were protogenetic inclusions present in the pegmatitic growth environment before the sapphire began to form. Raman microspectrometry analysis (figure 14) confirmed the identity of several crystal inclusions as pargasite.

The absence of 3309 peak series in IR spectroscopy and the microscopic observation of unaltered internal features supported an unheated call. The classic metamorphic UV-Vis absorption spectra, the metamorphic-type low-Fe chemistry data collected with LA-ICP-MS, and the observed inclusion scene supported a Kashmir origin conclusion. The issued GIA report identified the stone as a natural sapphire from Kashmir with no indications of heating.

Pargasite was once thought to be unique to Kashmir until it was found in sapphires from other countries. Nonetheless, pargasite inclusions are a strong indicator of Kashmir origin. With the support of advanced analytical instrumentation (UV-Vis and LA-ICP-MS) in addition to careful examination of the overall internal features (milky bands, ladder-like stringers, and snowflakes), the presence of pargasite inclusions can conclusively determine a Kashmir origin.

Jonathan Muyal

SYNTHETIC DIAMONDS

An Irradiated CVD Synthetic Melee Diamond Found in Irradiated Natural Melee Diamonds

Mixing of synthetic melee diamonds with natural melee diamonds has been reported several times. Those examples were colorless (Winter 2016 Lab Notes, pp. 416–417; Summer 2017 Lab Notes, pp. 236–237) and yellow (Winter 2014 Lab Notes, pp. 293–294). Recently, GIA's Tokyo lab found a single irradiated green-blue CVD synthetic melee diamond in a parcel of similarly colored irradiated natural melee.

The parcel of 300 uniformly green-blue round melee was submitted for identification (figure 15). Each diamond's color was attributed to strong

Figure 15. This group of 300 green-blue diamonds (1.97 carats total) was screened by GIA's Tokyo laboratory. Among these, 299 were irradiated natural melee diamonds and the one on the right was an irradiated CVD synthetic melee diamond.

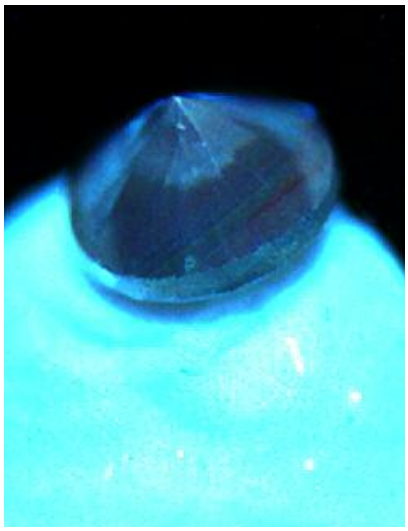

Figure 16. DiamondView imaging revealing weak linear striations in the pavilion of the irradiated CVD synthetic melee diamond.

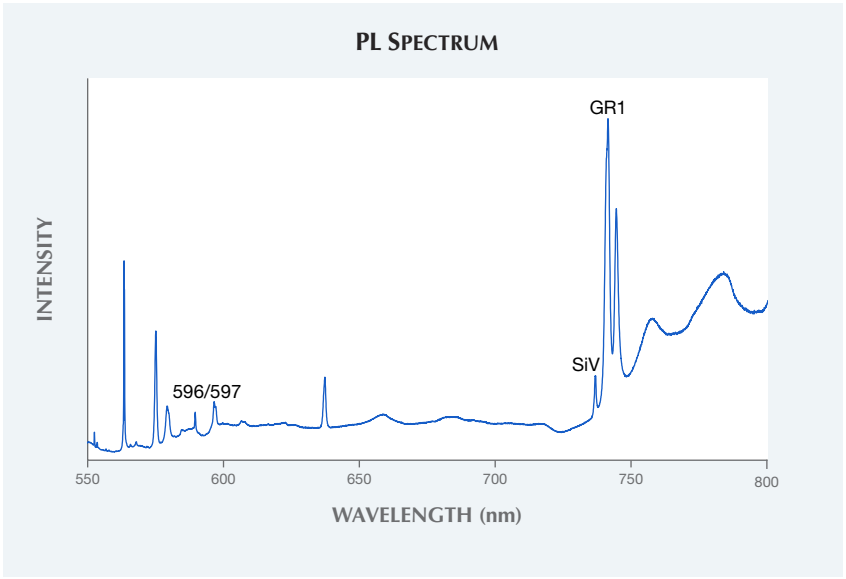

Figure 17. The photoluminescence spectrum of the green-blue CVD synthetic melee diamond at liquid nitrogen temperature shows a strong GR1 peak. The SiV^- center defect can be observed at around 736 nm. The doublet at 596/597 nm indicates that this diamond did not undergo annealing after synthesis.

GR1 by irradiation treatment. Infrared absorption spectroscopy, photoluminescence spectroscopy, and DiamondView analysis confirmed that 299 of them were irradiated natural diamonds and one of them was an irradiated CVD synthetic diamond. The CVD synthetic diamond weighed 0.007 ct, with a diameter of 1.14 mm.

DiamondView images of the synthetic showed very weak linear striations in the pavilion (figure 16). Dark inclusions were observed under the microscope. The infrared spectrum showed a peak at 3123 cm^{-1}, and the photoluminescence spectrum showed doublet peaks at 596/597 nm (figure 17). These peaks are seen in CVD synthetic diamonds without post-annealing. The photoluminescence spectrum also showed a small, broad SiV^- center defect at 737 nm next to a very strong GR1 center at 741 nm (figure 17). From the peak at 3123 cm^{-1} and the 596/597 nm doublet peak, this diamond was concluded to be irradiated without pre-annealing.

Irradiated CVD synthetic diamonds are rarely seen at GIA, which had examined only six of them before this report (Fall 2014 Lab Notes, pp. 240–241; Fall 2015 Lab Notes, pp. 320–321; Summer 2018 Lab Notes, pp. 215–216). Previously reported irradiated CVD synthetic diamonds were relatively large, from 0.43 to 1.34 ct. This is the first melee-sized irradiated CVD synthetic diamond examined by GIA.

Shoko Odake

Gemological Analysis of Lightbox CVD-Grown "White" Diamonds

Lightbox, a De Beers company, has begun selling "white," pink, and blue CVD laboratory-grown diamonds at a flat rate of $800 per carat. Through a third-party vendor, we recently had the opportunity to examine two such samples (0.24 and 0.26 ct) intended for setting in a pair of earrings. Both were near-colorless with color grades equivalent to G color and cut grades of Excellent and Very Good, respectively.

Both lab-grown diamonds had very few clarity characteristics. The 0.24 ct sample had a pinpoint in a bezel facet, and the 0.26 ct round (figure 18, left) had a feather in a star facet, both with VVS clarity. However, the grade-setting feature for both was the Lightbox logo, internally inscribed underneath the table facet (figure 18, center). As a result of the Lightbox mark, the clarity grade for both was reduced to VS. The laser-inscribed internal feature is reportedly made using technology developed by Opsydia (Gem and Jewellery Export Promotion Council, "De Beers to use Opsydia's laser tech to inscribe lab-grown diamonds in Lightbox Jewelry," https://www.gjepc.org/news_detail.php?id=4075). It is composed of dual narrow lines ~2.5 microns wide with a total area of 300 × 300 microns, positioned about 200 microns below the table surface.

Spectroscopic analysis showed both samples had very similar features that were consistent with previously analyzed CVD products from other manufacturers. IR absorption spectroscopy confirmed these samples as type IIa with no detectible single nitrogen at 1344 cm^{-1}. Photoluminescence (PL) spectra showed that both had the 596/597 nm doublet, indicating that they were as-grown and not subjected to post-growth HPHT processing (S. Eaton-Magaña and J.E. Shigley, "Observations on CVD-grown synthetic diamonds: A review," Fall 2016 *G&G*, pp. 222–

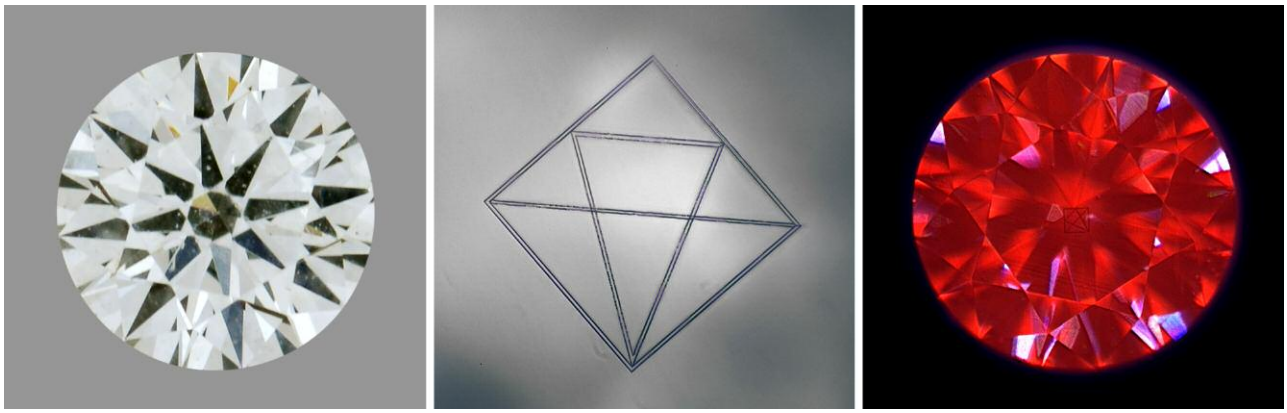

Figure 18. The 0.26 ct near-colorless CVD-grown diamond (left) has an internal inscription showing the Lightbox logo, composed of dual narrow lines. The logo is easily detected with a microscope (center) and clearly visible in the DiamondView image (right), in which the red fluorescence is due to nitrogen-vacancy centers. Also seen in the DiamondView image are subtle striations, additional evidence of the CVD origin. The outer square of the Lightbox logo measures 300 microns on each side.

245). Faceted, as-grown near-colorless CVD samples are less common since most manufacturers grow CVD layers quickly, but with a brown color, knowing that they can be HPHT treated to improve color appearance after growth. Approximately 75% of the CVD material in this color range examined by GIA has been HPHT treated after growth (S. Eaton-Magaña, "Summary of CVD lab-grown diamonds seen at the GIA laboratory," Fall 2018 *G&G*, pp. 269–270).

Through crossed polarizers, we observed very low birefringence compared with the majority of CVD-grown diamonds examined. Additionally, both samples showed very strong emission from nitrogen-vacancy centers by PL spectroscopy (figure 19), as well as visible red fluorescence using DiamondView imaging (figure 18, right), but there was no detectable fluorescence with long-wave UV. With careful DiamondView imaging, subtle CVD striations were visible through the table facet. In the DiamondView images, there were no apparent growth interfaces showing multiple growth events, and no apparent seed crystal remnants were observed. Also, PL spectroscopy of both samples showed very weak but detectable silicon-vacancy centers at 736.6/736.9 nm.

Figure 19. This 514 nm PL spectrum collected on the 0.26 ct sample at liquid nitrogen temperature shows strong nitrogen vacancy centers at 575 and 637 nm and the 596/597 nm doublet, evidence of an as-grown CVD sample.

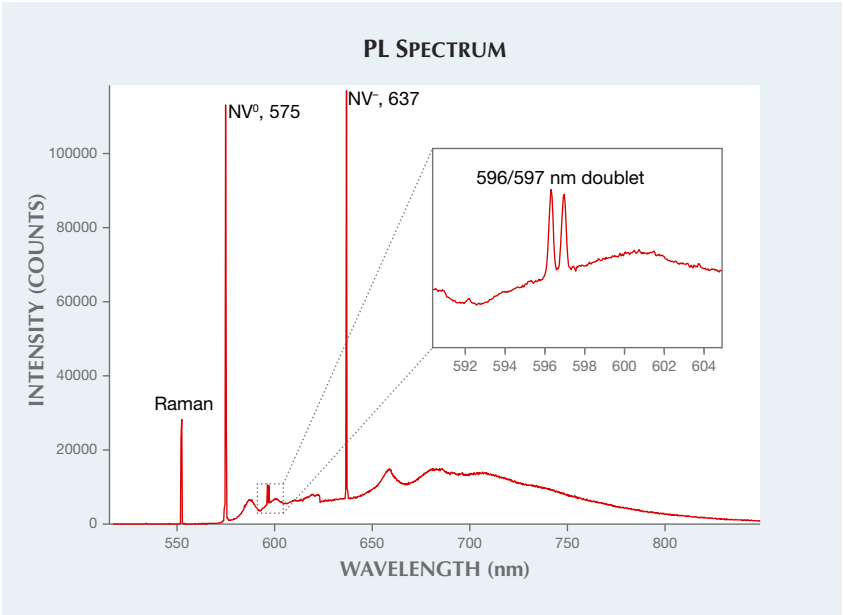

The Lightbox CVD lab-grown diamonds, due to their price point and manufacturer, will likely be highly visible in the trade. The pink and blue samples, as evidenced by De Beers' literature, have an appearance that is unusual among natural-color diamonds and are unlikely to ever be perceived as a natural-color product. However, the colorless Lightbox samples are readily identifiable as CVD-grown diamonds by spectroscopic techniques, DiamondView imaging, and their distinctive internal inscription.

Sally Eaton-Magaña

Cat's-Eye Brazilian Paraíba TOURMALINE

A vivid shade of tourmaline varying

Figure 20. This 0.51 ct Paraíba tourmaline from Brazil displays sharp chatoyancy.

from "neon" blue to greenish blue, caused by copper and manganese, was discovered in Brazil in the 1980s. Recognized as "Paraíba" tourmaline in the gem trade, it is still highly sought after, even though tourmalines exhibiting this "Paraíba" color are now more accessible from localities such as Nigeria and Mozambique.

Recently, GIA's Bangkok laboratory received a vivid blue tourmaline with chatoyancy (figure 20), weighing 0.51 ct and measuring 5.89 × 4.19 × 2.46 mm. Standard gemological testing resulted in a spot refractive index reading of 1.64 and a specific gravity of 3.05. Microscopic examination revealed diagnostic irregular two-phase inclusions, trichites, and acicular (needle-like) features. The sharp cat's-eye effect was caused by an included layer of fine parallel growth tubes positioned just above the base of the cabochon. The phenomenon of chatoyancy enhances its rarity and value.

LA-ICP-MS was used to perform an elemental analysis. The sample showed high Cu ranging from 7289 to 10544 ppmw, as well as 9494–10441 ppmw Mn, 114–133 ppmw Ga, 55–65 ppmw Pb, 39–48 ppmw Fe, 14–20 ppmw Zn, and 0.6–0.5 ppmw Sr. The very high concentration of Cu as well as the results for Ga (<250 ppmw), Pb (<100 ppmw), and Sr (<10 ppmw) supported its Brazilian origin (J.E. Shigley et al., "An update on 'Paraíba' tourmaline from Brazil," Winter 2001 *G&G*, pp. 260–267; A. Abduriyim et al., "Paraíba-type copper-bearing tourmaline from Brazil, Nigeria, and Mozambique: Chemical fingerprinting by LA-ICP-MS," Spring 2006 *G&G*, pp. 4–21; Z. Sun et al., "A simplified species classification for gem-quality tourmaline by LA-ICP-MS," submitted for publication). Copper-bearing tourmaline of this color is typically referred to in the trade as "Paraíba" tourmaline.

Cat's-eye Paraíba tourmaline is not new, though fewer than 10 have been submitted to GIA laboratories. The combination of well-developed chatoyancy, transparency, pleasing vivid blue color, and Brazilian origin make this a rare and noteworthy gemstone.

Vararut Weeramongkhonlert

PHOTO CREDITS

Robison McMurtry—1, 5, 11, 18 (left); Garrett McElhenny—2, 3; Nicole Ahline—4; Hollie McBride—6; Sood Oil (Judy) Chia—7; Joyce Wing Yan Ho—8; Claire Malaquias—10; Towfiq Ahmed—12; Jonathan Muyal—13; Shunsuke Nagai—15; Sally Eaton-Magaña—18 (center and right); Nuttapol Kitdee—20